A General Approach for Predicting the Filtration of Soft and Permeable Colloids: The Milk Example

Antoine Bouchoux,*[,†,‡,⊥] Peng Qu,[†,‡] Patrice Bacchin,[§,∥] and Geneviève Gésan-Guiziou[†,‡]

[†]INRA, UMR 1253 Science et Technologie du Lait et de l'Œuf, F-35042 Rennes, France

[‡]AGROCAMPUS OUEST, UMR1253 STLO, F-35042 Rennes, France

[§]Université de Toulouse, INPT, UPS, Laboratoire de Génie Chimique, 118 Route de Narbonne, F-31062 Toulouse, France

[∥]CNRS, UMR 5503, F-31062 Toulouse, France

ABSTRACT: Membrane filtration operations (ultra-, microfiltration) are now extensively used for concentrating or separating an ever-growing variety of colloidal dispersions. However, the phenomena that determine the efficiency of these operations are not yet fully understood. This is especially the case when dealing with colloids that are soft, deformable, and permeable. In this paper, we propose a methodology for building a model that is able to predict the performance (flux, concentration profiles) of the filtration of such objects in relation with the operating conditions. This is done by focusing on the case of milk filtration, all experiments being performed with dispersions of milk casein micelles, which are sort of "natural" colloidal microgels. Using this example, we develop the general idea that a filtration model can always be built for a given colloidal dispersion as long as this dispersion has been characterized in terms of osmotic pressure Π and hydraulic permeability k. For soft and permeable colloids, the major issue is that the permeability k cannot be assessed in a trivial way like in the case for hard-sphere colloids. To get around this difficulty, we follow two distinct approaches to actually measure k: a direct approach, involving osmotic stress experiments, and a reverse-calculation approach, that consists of estimating k through well-controlled filtration experiments. The resulting filtration model is then validated against experimental measurements obtained from combined milk filtration/SAXS experiments. We also give precise examples of how the model can be used, as well as a brief discussion on the possible universality of the approach presented here.

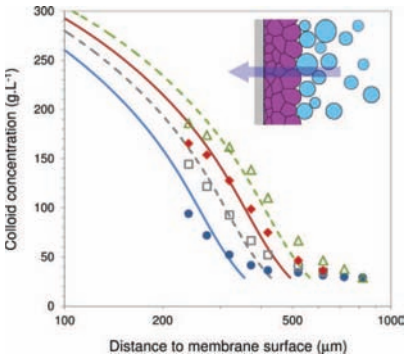

1. INTRODUCTION

Membrane operations like ultra- or microfiltration are now extensively used in the industry for separating and/or concentrating colloidal particles (colloidal humic matter, mineral colloids, macromolecular drugs, proteins, etc.). In the past twenty years, considerable research effort has been devoted to understanding and modeling such filtration operations.[1] However, current approaches are still limited to monodisperse hard-sphere colloids, while the colloids encountered in the real world are often polydisperse, soft, deformable, and even porous. In this paper, we treat the generic problem of soft and permeable colloids, with the objective of proposing a methodology for building a filtration model for such objects.

Our experimental model system is the milk casein micelle, which is a "natural" equivalent to the artificial colloidal microgels that are now commonly used in the Soft Matter community (like poly(*N*-isopropylacrylamide) (PNIPAM) systems, for instance).[2,3] Those micelles, which make up to 80% of the protein content of cow milk, are complex association colloids made of four distinct caseins (α_{s1}, α_{s2}, β, and κ) and 8% in mass of phosphate and calcium ions.[4] They are highly polydisperse, with a vast majority of micelles with diameters between 50 and 200 nm.[5,6] Because they contain a lot of water in their internal core (about 76%), the casein micelles can literally be viewed as sponge-like colloids or microgels that are highly porous (and consequently permeable), and that can deform when compressed.[5,7−10] The choice of the casein micelle is also motivated by the fact that milk filtration operations are widely encountered in the dairy industry,[11,12] and it is now well established that the performance of ultra- and microfiltration in dairy processing are intimately linked to the presence of the casein micelles in milk and to their accumulation near the membrane surface.[13] A filtration model would then be of considerable interest and benefit to this industry.

Since the pioneering works of Cohen and Probstein,[14] and later of Belfort et al. and Bowen et al.,[15,16] understanding and modeling the filtration of a colloidal dispersion has always been a challenge. We refer the reader to the review of Bacchin et al. for a detailed discussion and some historical considerations on

that point.[17] Also, some other key references can be cited here, like those of Chen et al. and Elimelech et al., for instance.[18−21] In brief, the particularity of colloidal filtration is that the interactions between and within the objects have dominant effects on the filtration performance,[14] whereas hydrodynamic/shear-induced interactions are prevailing when filtrating micrometer-size particles.[22] As a consequence, colloidal interactions have to be taken into account in a modeling approach. In latest developments, this is usually done through the use of the osmotic pressure Π as a quantitative descriptor of the colloidal interactions.[16,23,24] The osmotic pressure of a colloidal dispersion indeed reflects the balance of all interactions in the system.[25−28] It gives a measure of how the dispersion resists to an overall increase in its concentration: the higher its osmotic pressure, the harder it is to "compress" it. Besides osmotic pressure, another essential parameter that is necessary to accurately model the filtration of a colloidal dispersion is its permeability k, which measures the resistance of the system to the hydraulic flow that passes through it.[29,30] As opposed to the osmotic pressure, k is a "structural" parameter that originates from the hydrodynamic drag forces exerted on the involved colloids and that is therefore directly related to their size and spatial organization.[30,31] Of course, Π and k are both concentration-dependent parameters, and it is by knowing how Π and k evolve with concentration C for a given colloidal dispersion that the filtration model can be built.[16,32] The model can then be used in several ways, like predicting concentration profiles and permeation volumes or fluxes versus time (note that a model of this type has been recently used for describing the concentration of colloids in microevaporators, in direct analogy with filtration[33]).

This modeling approach has now been used for quite a number of colloidal objects, such as latex particles or globular proteins.[1,16,23,34,35] The way the authors deal with the osmotic pressure and its variation with concentration varies from case to case. In some studies, the $\Pi(C)$ relation is measured experimentally, using the osmotic stress technique for instance.[34,35] In other studies, the authors use theoretical expressions for $\Pi(C)$, those expressions often being based on the DLVO theory and therefore, depending on the size, the surface charge and some other properties of the colloid.[1,16,23] On the other hand, for all the systems investigated so far, $k(C)$ is always taken as the theoretical permeability of a bed of noninteracting and nonporous hard spheres of size equivalent to the size of the colloid investigated. Mathematical expressions like the one of Happel are the most often used to estimate this permeability.[1,16,34,35] In such expressions, $k(C)$ is only related to the size of the colloid and to the volume fraction occupied by the colloid in the dispersion.[36]

In the cases investigated, the use of such theoretical expressions is possible because latex particles and globular proteins are, like hard spheres, nondeformable and nonpermeable. One clearly sees here that this approach cannot be followed entirely for soft and permeable objects. Indeed, while it is always possible to measure $\Pi(C)$ for any dispersion of soft colloids (and casein micelle dispersions in particular; see section 4.1), it is much more difficult to know how $k(C)$ varies with C in such a case. As opposed to hard spheres, which are nonpermeable objects that can pack to a maximum volume fraction of ∼0.64 for the monodisperse case, deformable and porous particles can pack to concentrations that are much higher than the concentration for close-packing. Moreover, in these conditions of high concentrations, it is the internal porosity of the objects that determines the permeability of the dispersion. In such a case, $k(C)$ is very difficult—if not impossible—to predict theoretically. With the present study, and taking the casein micelle as our model experimental system, our objective is to get around this difficulty and finally provide a model that is fully able to predict the filtration of a dispersion of soft and permeable colloids. Two approaches are presented for estimating $k(C)$. The first one consists of measuring $k(C)$ experimentally through specifically designed osmotic stress experiments. The other one, inspired from the work of Bowen et al.,[1,37] consists of estimating $k(C)$ from dead-end filtration runs and from the known variation of Π with C.

As a final note, we emphasize that this work is dedicated to the dead-end filtration case only, and has to be considered as a first step toward the building of a model for industrial cross-flow filtrations. This last case, for which the effect of cross-flow velocity on the build-up of the accumulated layer needs to be taken into account, will be investigated in future studies.

2. THEORY

2.1. Filtration Model. Figure 1 gives a schematic view of how deformable colloids accumulate at a membrane surface in dead-end filtration. The objects are of course the most concentrated at the membrane surface. In the depicted situation, the local concentration is such that the colloids are deformed and in contact with each other. In the case of casein micelles, this corresponds to the formation of a gel or irreversible deposit.[13,38−40] Above this very dense layer, a polarized layer exists, where the objects are still more concentrated than in the bulk but where phase transition has not yet occurred. This phase transition can be characterized through a critical osmotic pressure Π_{crit}, as depicted in Figure 1.

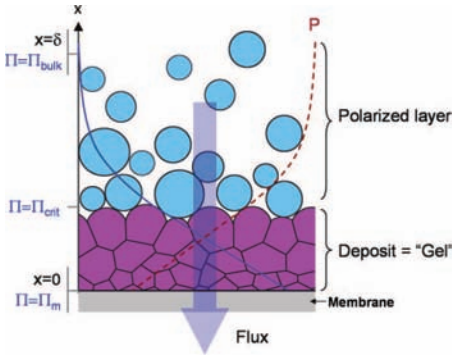

Figure 1. Schematic cartoon of soft colloidal particles accumulating at a membrane surface in dead-end filtration. The full and dashed lines illustrate how the osmotic pressure $\Pi(C)$ and the hydrostatic pressure P vary through the polarized layer and the deposit. At $\Pi(C) > \Pi_{crit}$, the polarized layer turns into an irreversible deposit that does not disperse when pressure is released.[40]

Let us first consider the polarized layer only. In this layer, the solvent flux is governed by the solution thermodynamics. The effective driving force for permeation through the polarized layer is then simply the difference in osmotic pressure Π at its two ends.[19,41] At steady state, and with the convention of Figure 1, this gives the following expression for the absolute value J of the solvent volumetric flux at any point of the polarized layer

$$J = -\frac{1}{\eta R_{PL}}\frac{\mathrm{d}\Pi}{\mathrm{d}x} = -\frac{k_{PL}}{\eta}\frac{\mathrm{d}\Pi}{\mathrm{d}x} \tag{1}$$

where R_{PL} is the resistance of the polarized layer to solvent flow at position x, $k_{PL} = 1/R_{PL}$ is the corresponding permeability of the polarized layer toward the solvent, and η is the dynamic viscosity of the solvent.

As it was carefully demonstrated by Elimelech et al.,[19] the osmotic pressure difference across the polarized layer is in fact strictly equivalent to the cumulative hydrodynamic drag forces exerted on the particles. This implies that eq 1 can be expressed in terms of a hydraulic pressure drop across the polarized layer, the hydraulic resistance R and the permability k being defined in the exact same way. This is the well-known Darcy's law that is commonly used in filtration theory

$$J = \frac{k_{PL}}{\eta}\frac{\mathrm{d}P}{\mathrm{d}x} \tag{2}$$

Let us now consider the gel layer. In that case, and like in the case of any porous media, the classical cake filtration theory directly applies. The permeation flux through the gel is then expressed in the same form as eq 2

$$J = \frac{k_{\mathrm{GEL}}}{\eta}\frac{\mathrm{d}P}{\mathrm{d}x} \tag{3}$$

In cake filtration theory, the so-called "solid" (or compressive, or effective) pressure P_S is usually introduced at that point.[42−44] This pressure reflects the "stress within the matrix of solid particles" that make the cake.[43] For a gel or a packing of microgel beads such as casein micelles, the effective pressure is nothing other than the osmotic pressure Π of the medium.[28,45] The same equivalence as the one demonstrated by Elimelech et al.[19] in the polarized layer can then be used for the gel/cake phase.[42−44,46] This results in

$$\frac{\mathrm{d}P}{\mathrm{d}x} = -\frac{\mathrm{d}\Pi}{\mathrm{d}x} \tag{4}$$

in all positions of the gel. In other words, a drop in liquid pressure within the gel is always exactly balanced by an increase in osmotic pressure.

Quite naturally, eqs 3 and 4 then give

$$J = -\frac{k_{\mathrm{GEL}}}{\eta}\frac{\mathrm{d}\Pi}{\mathrm{d}x} \tag{5}$$

which is the exact homologue of eq 1 but in the gel phase.

Thus from eqs 1 and 5, one can see that the permeation flux J, at steady state, can be described by the same single equation over the entire layer of material accumulated at the membrane surface, i.e., the polarized layer plus the gel layer. Taking explicitly into account the concentration dependence of both k and Π, this equation writes

$$J = -\frac{k(C)}{\eta}\frac{\mathrm{d}\Pi(C)}{\mathrm{d}x} \tag{6}$$

Equation 6 is the key equation used in the present work. It basically says that the filtration flux of a colloidal dispersion can be predicted knowing the variations of permeability and osmotic pressure with the concentration of colloids. Quite importantly, we believe that eq 6 is universal and can be applied to any colloidal dispersion, including "complicated" ones such as mixtures of several colloids and/or dispersions of soft colloids, for instance. In other words, it is possible from eq 6 to predict a filtration flux of any colloidal dispersion as long as $k(C)$ and $\Pi(C)$ are known. Note that, for monodisperse hard-sphere colloids, we can actually demonstrate that the "generalized Darcy's law" of eq 6 is in fact equivalent to the convection−diffusion mass balance equation that is generally used for describing the concentration polarization phenomenon in such a peculiar case.[1,16,23,32] We briefly discuss that point in the Supporting Information provided with this article.

As a side note, it is important to stress here that electroviscous effects can somewhat increase the apparent viscosity of the fluid at sufficient colloid concentrations (see ref 47 for details). This can be accounted for through an additional term in eq 6.[16] However, we voluntarily neglect those effects, as they are known to be minor in most cases (×1.4 at max).

2.2. Modeling the Filtration from $k(C)$ and $\Pi(C)$. In dead-end filtration, the prediction of a flux from $k(C)$ and $\Pi(C)$ relies on a series of hypotheses and calculations that are given in detail in the papers of Bowen's and Bacchin's groups,[1,16,23] and that we just briefly give here.

First, the quasi-stationary approximation is applied, meaning that the filtration is considered as a succession of stationary states for which eq 6 can be used as such. Multiplying eq 6 by C, we obtain

$$JC\mathrm{d}x = -\frac{k(C)C}{\eta}\mathrm{d}\Pi(C) \tag{7}$$

We then integrate eq 7 on the thickness δ of the accumulated layer

$$\int_0^\delta JC\mathrm{d}x = -\int_0^\delta \frac{k(C)C}{\eta}\mathrm{d}\Pi(C) \tag{8}$$

which simplifies in

$$J\int_0^\delta C\mathrm{d}x = \int_{\Pi_{\mathrm{bulk}}}^{\Pi_m} \frac{k(C)C}{\eta}\mathrm{d}\Pi \tag{9}$$

We now make the reasonable assumption that the full quantity of matter accumulated (polarized layer + gel, first integral in eq 9) is directly related to the filtered volume V_f and the bulk concentration of colloids C_{bulk}. We then have

$$JC_{\mathrm{bulk}}\frac{V_f}{A_m} = \int_{\Pi_{\mathrm{bulk}}}^{\Pi_m} \frac{k(C)C}{\eta}\mathrm{d}\Pi \tag{10}$$

$$V_f = \frac{A_m}{JC_{\mathrm{bulk}}\eta}\int_{\Pi_{\mathrm{bulk}}}^{\Pi_m} k(C)C\mathrm{d}\Pi \tag{11}$$

with A_m the membrane area.

The Darcy's law, expressed at the membrane surface, is also important since it directly relates J to the osmotic pressure Π_m at the membrane surface

$$J = \frac{\Delta P - \Pi_m}{\eta R_m} \tag{12}$$

with R_m the hydraulic resistance of the membrane.

Then, for a given transmembrane pressure ΔP, the calculation of V_f and J with filtration time t consists of the following steps: (a) Assume a given value of C_m, the concentration at the membrane surface. (b) Calculate Π_m knowing the relation between Π and C. (c) Calculate J from eq 12, knowing the membrane resistance. (d) Calculate V_f from eq 11, the integral term being estimated through either a numerical or graphical method and using the known variations

of $k(C)$ and $\Pi(C)$. (e) Reiterate steps (a)−(d) for other values of C_m covering the expected range of variation (from C_{bulk} to a realistic maximum value of C that can be attainable at the membrane surface). (f) When the values of V_f and J are known for a sufficient number of points, the time t necessary to filtrate one given volume V_f can be estimated through the following simple integration, again performed either numerically or graphically

$$t = \int_0^{V_f} \frac{1}{A_m J} \mathrm{d}V \tag{13}$$

By performing step (f) for a number of points, we obtain the full variation of V_f and J with filtration time t.

Additional information that can be obtained at this point is the concentration and osmotic pressure profiles in the accumulated layer. To obtain those profiles, one first has to choose a filtration time t, which implies setting both a colloid concentration C_m and an osmotic pressure Π_m at the membrane surface (see preceding calculation). The C and Π profiles are then simply constructed by solving the following integral at different positions in the layer

$$x = \frac{1}{\eta J} \int_{\Pi}^{\Pi_m} k(C) \mathrm{d}\Pi \tag{14}$$

This whole approach has been followed in some previous filtration studies involving dispersions of one "hard" (nondeformable) and nonporous colloid, like latex particles, for instance.[1,16,23,34,35] In all cases, $k(C)$ is simply assumed to be the permeability of a bed of nonporous spheres, and is estimated through known mathematical expressions such as the Happel's equation.[36] Concerning $\Pi(C)$, theoretical expressions also exist for different colloidal systems: from the simple expressions of Carnahan−Starling for dispersions of noninteracting hard spheres to the more complicated DLVO-based expressions proposed by Bowen et al. for dispersions of interacting spheres.[1,48] However, as far as a given colloidal system is concerned, and when it is possible, our advice is to determine experimentally the $\Pi(C)$ curve, since accurate osmotic pressure models are still lacking.[26,27] Such an experimental determination of $\Pi(C)$ is usually performed through the osmotic stress technique.[25,34,49]

2.3. Using the Model in a Reverse Way: Estimating $k(C)$ Knowing $\Pi(C)$ and $J(t)$. In this paper, we deal with dispersions of casein micelles, which are sponge-like objects that are both porous and deformable.[5,7−10] As for other colloids, it is possible to determine the $\Pi(C)$ behavior of casein micelle dispersions through osmotic stress experiments (section 4.1 and ref 9). On the other hand, the $k(C)$ of casein micelle dispersions is both difficult to measure experimentally (last part of section 3.3) and nearly impossible to predict theoretically: mathematical expressions exist for dispersions of porous spheres,[30,50] but they are still impractical as they rely on internal characteristics that are not known yet for casein micelles.

We propose here to estimate the $k(C)$ of casein micelle dispersions by using the filtration model of section 2.1 "reversely". That is to say, we propose to estimate $k(C)$ using $\Pi(C)$, known experimentally, and values of $J(t)$, also obtained experimentally through well-defined filtration runs. After $k(C)$ is determined in that way, our idea is that the knowledge of $k(C)$ and $\Pi(C)$ will make it possible to predict the filtration of casein micelle dispersions in absolutely any conditions of filtration, simply by following the steps (a)−(f) found in the previous section. In many aspects, this proposition is similar to the one of Bowen et al. in 2001, who showed that it is possible to obtain $\Pi(C)$ for a protein dispersion, still using the model presented in section 2.1, but this time taking the Happel's equation for $k(C)$, and using $J(t)$ values obtained through dead-end filtration experiments.[37] In both cases (estimating $k(C)$ from $\Pi(C)$ and $J(t)$, or estimating $\Pi(C)$ from $k(C)$ and $J(t)$), the calculations are based on eq 10, which can be rewritten in the form

$$JV_f = \frac{A_m}{C_{bulk}\eta} \int_{\Pi_{bulk}}^{\Pi_m} k(C) C \mathrm{d}\Pi \tag{15}$$

This equation can then be turned into the following time-dependent expression (see ref 16 for a detailed description of the mathematical manipulations that are performed)

$$JV_f = \frac{A_m}{C_{bulk}\eta} \int_0^t k(C_m) C_m \frac{\mathrm{d}\Pi_m}{\mathrm{d}t} \mathrm{d}t \tag{16}$$

which gives, after differentiation

$$A_m J^2 + V_f \frac{\mathrm{d}J}{\mathrm{d}t} = \frac{A_m}{C_{bulk}\eta} k(C_m) C_m \frac{\mathrm{d}\Pi_m}{\mathrm{d}t} \tag{17}$$

When differentiated with respect to time, eq 12 gives

$$\frac{\mathrm{d}J}{\mathrm{d}t} = -\frac{1}{\eta R_m} \frac{\mathrm{d}\Pi_m}{\mathrm{d}t} \tag{18}$$

Then, by combining eqs 17 and 18, we obtain

$$k(C_m) C_m = -\frac{C_{bulk}\left(A_m J^2 + V_f \frac{\mathrm{d}J}{\mathrm{d}t}\right)}{A_m R_m \frac{\mathrm{d}J}{\mathrm{d}t}} \tag{19}$$

Thus, by performing filtration experiments where V_f, and consequently J, are obtained as a function of time, we can simultaneously: (i) calculate the osmotic pressure at the membrane surface Π_m as a function of time using eq 12, and then determine the corresponding C_m at each time, and (ii) calculate the product $k(C_m)C_m$ as a function of time using eq 19. The permeability $k(C)$ is then obtained by computing the C_m and $k(C_m)C_m$ values at each time.

3. EXPERIMENTAL SECTION

3.1. Dispersions. All dispersions were prepared from native phosphocaseinate powder (NPC) dispersed in a solvent made from ultrafiltration of skimmed milk (UF permeate). The NPC powder was prepared in our laboratory following a protocol given by ref 51 and that we summarize in a previous paper.[40] In the powder, the caseins and their associated minerals make more than 90% of the total solid content.

The UF permeate solvent was prepared through membrane ultrafiltration of fresh skim milk (5000 Da cutoff). The totality of the milk protein fraction, i.e., caseins and whey proteins, is eliminated through this operation. The UF permeate contains the milk minerals, lactose, and a few other low molar mass molecules.[52] Both thiomersal and sodium azide, purchased from Sigma-Aldrich (St. Louis, MO, USA), were added to the NPC dispersions as preservatives at 0.02% and 0.05% (w/w), respectively.

NPC dispersions with concentrations ranging from 1 to 120 g·L^{-1} were prepared by thoroughly mixing the NPC powder in UF permeate for 15 h at 35 °C, a condition that ensures full dissolution of the powder.[53] For higher concentrations, additional NPC powder was added into a dispersion of 120 g·L^{-1} and mixed for another 24 h at 35

°C. The method allows making NPC dispersions up to 180 g·L^{-1} in concentration.

In NPC dispersions, the casein micelles are known to be in a structural state that is virtually identical to their native state in milk.[54] Also, NPC dispersions have the exact same pH and ionic strength as fresh skim milk, i.e., pH 6.7 ± 0.1 (20 °C) and ionic strength 80 mM. In those conditions, the casein micelles are very stable, predominantly because of the brush repulsion forces exerted by the ∼10 nm κ-casein chains that protrude from their surface.[55,56]

3.2. Osmotic Pressure Measurements. *Osmotic Stress.* The osmotic pressure of NPC dispersions at concentrations ranging from 30 to 700 g·L^{-1} was measured using osmotic stress. This technique is based on water exchange between the sample and a polymer solution of controlled osmotic pressure.[25,49] The sample (NPC dispersion) is placed in a dialysis bag that, in turn, is immersed in a reservoir containing a polymer solution (poly(ethylene glycol), PEG, in our case) also prepared with UF solvent. At equilibrium, i.e., after at least 14 days of compression, the chemical potentials of water on either side of the bag are equal, and therefore the osmotic pressure of the sample equals that of the polymer in the reservoir. The casein concentration in the bag is then determined through drying at 105 °C, thus giving one point $\Pi(C)$ of the osmotic pressure curve.

Experimentally, the osmotic stress was realized using standard regenerated cellulose Spectra/Por 2 dialysis bags with a molecular weight cutoff of 12−14 kD (Spectrum Laboratories, Rancho Dominguez, CA). These bags were chosen to allow exchange of water, ions, and lactose, but not caseins or PEG. Two types of stressing polymers were used: a 20 kD and a 35 kD molecular weight PEG. Because of their size, those PEG molecules are supposed not to pass through the dialysis bags of 12−14 kD (even if "reptation" events cannot be excluded; see next paragraph). Solutions of PEG were prepared at different osmotic pressures by dispersing the PEG polymer in UF permeate. For both solutions, the relation between osmotic pressure Π (bar) and PEG concentration [PEG] (%, w/w) is expressed as follows[9,57]

$$\log(\Pi \times 10^5) = A + B[\mathrm{PEG}]^C \tag{20}$$

with $A = 0.49$, $B = 2.5$, and $C = 0.24$ for PEG 35 kD, and $A = 0.57$, $B = 2.75$, and $C = 0.21$ for PEG 20 kD.

PEG 35 kD was used to prepare stressing solutions at pressures from 1000 Pa to a maximum of 4 bar, i.e., a pressure that corresponds to the maximum of solubility for this polymer in an aqueous solvent. PEG 20kD, which has a much higher solubility, was used to prepare stressing solutions at pressures ranging from 5 to 100 bar. We preferred to use two PEG molecules, and not only PEG 20 kD, for preparing our solutions because of the proximity between 20 kD molecular mass and the 12−14 kD cutoff of the dialysis membrane (lower cutoff are available, but with a much lower permeability). At pressures higher than 5 bar, this proximity is not a problem since the NPC dispersions are solid gels, thus ensuring that the possible migration/reptation of PEG molecules into the bags is strongly limited. At lower pressures, such a phenomenon cannot be excluded, and that is why we used a polymer of higher molecular mass (35 kD) in this case.

Membrane Osmometry. The osmotic pressure of NPC dispersions was also measured using a membrane osmometer. The instrument we used (Osmomat 090, Gonotec, Berlin, DE) is limited to low osmotic pressures (<7000 Pa), which correspond to the pressures measured for NPC dispersions with casein concentrations ranging from 1 to 180 g·L^{-1}.

A membrane osmometer is composed of two compartments of constant volumes that are separated by a membrane of a given molecular weight cutoff. The sample is introduced in one compartment, while the solvent (UF permeate in our case) is introduced in the other compartment. The induced osmotic pressure difference is then directly measured via a pressure transducer placed in the solvent side. For making our experiments, we used a 10 kD regenerated cellulose membrane supplied by Gonotec. Also, we performed experiments with either "fresh" (= freshly prepared, 0 day) or "aged" (14 days) NPC dispersions to examine the impact of casein proteolysis on osmotic pressure (section 4.1).

3.3. Permeability Measurements. *From Dead-End Filtration Runs.* The filtration apparatus we used is depicted in Figure 2. It

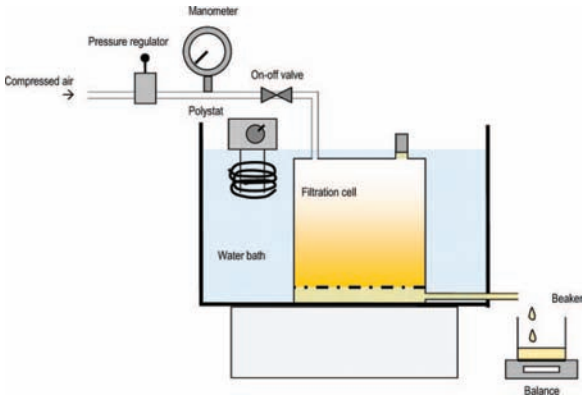

Figure 2. Schematic diagram of the dead-end filtration apparatus.

consists of a cell filtration of volume 2500 mL (model 2000, Millipore, Billerica, MA, USA) that accepts membranes with an effective area of 165 cm^2. Experiments were all performed with regenerated cellulose ultrafiltration membranes of 10 kD MWCO (Ultracel membrane, Millipore). Before each experiment, the hydraulic resistance R_m of the membrane was determined by filtering pure UF permeate. Note that the flux was always fully recovered (±5%) after each experiment and extensive membrane flushing; indicating that membrane internal fouling was negligible and that R_m can be considered constant during the course of the filtration.

All filtration experiments were performed with 1 g·L^{-1} NPC dispersions. We chose such a low concentration, which is more dilute than that of casein in milk (∼25 g·L^{-1}), to determine the permeability in a concentration range that also covers the very dilute regime. The dispersions were filtered under constant applied pressures ranging from 0.1 to 4 bar. The permeate solvent was collected in a beaker placed on an electronic balance linked to a computer, allowing the weight of permeate to be collected with time. All filtrations were performed at 20 °C, the filtration cell being immersed into a water bath at a controlled temperature.

The weight of permeate was converted into a volume knowing the density of UF permeate (ρ_{UF} = 1023 kg.m^{-3}, determined using a DMR 48 density meter, Anton Paar, AU). The filtration flux was then calculated by differentiating the volume data versus time, using Taylor's expressions like those given by Bowen et al.[37]

From Osmotic Stress Experiments. Imagine an infinite "slice" of NPC dispersion, the casein concentration in this slice being uniform and constant at C_{slice}. The thickness of the slice is e, and we assume that a hydrostatic pressure difference ΔP is applied through the slice. The resulting hydraulic flux would then simply be

$$J = \frac{k(C_{slice})}{\eta}\frac{\Delta P}{e} \tag{21}$$

By performing such an experiment with slices of different concentrations, it is theoretically possible to build the k(C) curve for NPC dispersions. Of course, it is difficult to do such a "perfect" experiment in the real world. There is, however, one way to approach the ideal conditions of the "slice experiment". The whole idea is based on the osmotic stress principle explained in section 3.2. An NPC dispersion is first equilibrated at a given osmotic pressure Π through osmotic stress (Figure 3a, left cartoon). After equilibrium is reached, the casein concentration in the bag is uniform. The bag is then placed in a reservoir of osmotic pressure Π + ΔΠ, ΔΠ being only a small pressure increment compared to Π. Because of the difference in osmotic pressure between the bag and the reservoir, the NPC

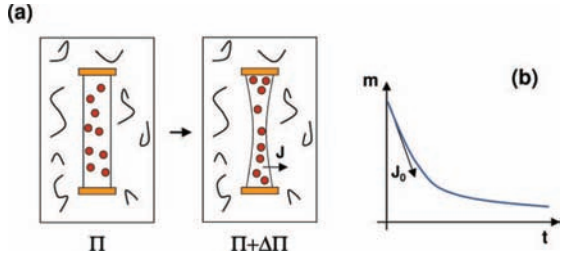

Figure 3. Determination of permeability $k(C)$ from osmotic stress experiments.

dispersion in the bag will compress to a higher concentration (Figure 3a).

During this compression, the mass of the bag is followed by weighing at different times. From these masses, it is then possible to obtain the flux J_0 of solvent that escapes from the bag at $t = 0$ (Figure 3b). Following eq 21, and neglecting the hydraulic resistance of the bag, this flux can be expressed as

$$J_0 = \frac{k(C_{\mathrm{bag},t=0})}{\eta}\frac{(\Pi_{\mathrm{reservoir}} - \Pi_{\mathrm{bag},t=0})}{e_{t=0}} = \frac{k(C_{\mathrm{bag},t=0})}{\eta}\frac{\Delta\Pi}{e_{t=0}} \tag{22}$$

with $e_{t=0}$ the thickness of the equivalent "slice". As a first approximation, it can be estimated as the volume of the bag V_{bag} divided by its surface A_{bag}

$$e_{t=0} = \frac{V_{\mathrm{bag}}}{A_{\mathrm{bag}}} = \frac{\rho_{\mathrm{cas}} M_{\mathrm{cas}}}{A_{\mathrm{bag}}} \tag{23}$$

where M_{cas} is the total mass of casein in the bag, as determined through drying at 105 °C after the experiment. ρ_{cas} is the density of the casein dispersion, calculated knowing $C_{\mathrm{bag},t=0}$ and using a density calibration curve determined from measurements performed beforehand (DMR 48 density meter, Anton Paar, AU).

From eqs 22 and 23, it is then possible to calculate the permeability k at casein concentration $C_{\mathrm{bag},t=0}$. Note that this method is only valid at time $t = 0$ since it is the only moment where the concentration in the bag (and consequently the permeability) can be considered uniform. Indeed, as compression occurs, colloidal reorganizations in the bag most probably happen. This leads to temporary structural inhomogeneities that prevent consideration of a uniform permeability in the bag. Note also that such experiments are difficult to prepare and perform, so that we only show here the results of 4 of them.

4. RESULTS AND DISCUSSION

4.1. Osmotic Pressure Π(*C*). Figure 4 gives the osmotic pressures measured for the NPC dispersions used in this work. The results obtained from osmotic stress combine two sets of data that were acquired by two distinct individuals at an interval of several years (this work and ref 9). As already pointed in the Experimental Section, 14 days of compression was required to reach thermodynamic equilibrium in those experiments. On the other hand, the membrane osmometry experiments were performed for the purpose of the present study only. In membrane osmometry, it takes between a few minutes and one hour of equilibration to get one point. Using this technique, it was then possible to measure the osmotic pressure of a "fresh" NPC dispersion (just after preparation) and of the same dispersion but after 14 days at ambient temperature.

For the purpose of the following discussion, it is useful to know the effective volume fraction ϕ that is occupied by the casein micelles at different casein concentrations. ϕ is simply calculated through

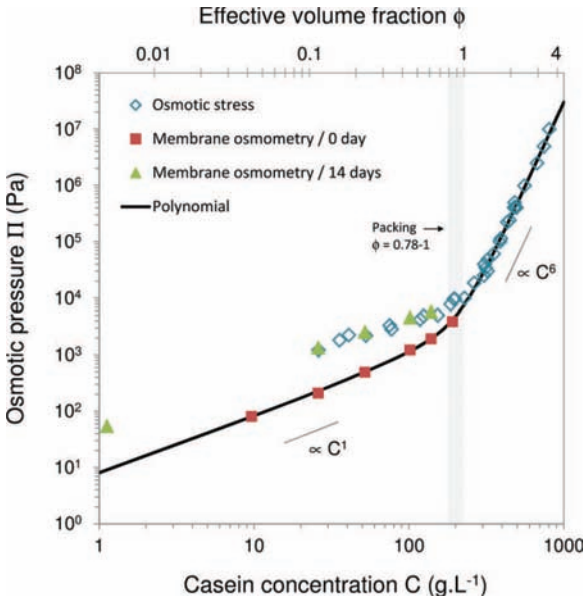

Figure 4. Evolution of osmotic pressure Π as a function of casein concentration and effective volume fraction. The open diamonds are the experimental points obtained through osmotic stress experiments (present work and ref 9). The full symbols are the experimental points obtained through membrane osmometry with either fresh (squares) or aged (triangles) NPC dispersions. The full line is eq 26.

$$\phi = \nu C \tag{24}$$

with ν the initial "voluminosity" ν of the micelle, taken as ν = 4.4 mL per gram of caseins.[6] ϕ is displayed on the top x-axis of Figure 4.

Looking at Figure 4, one can easily observe that osmotic pressure evolves differently with C at low and high casein concentrations. This two-regime behavior is a feature that we already report and discuss in a previous paper.[9]

In the low concentration regime (C < 180 g·L^{-1}), the osmotic pressure is directly proportional to the concentration of casein ($\Pi \propto C^1$, Figure 4). In this regime, we previously demonstrated through precise rheological measurements that the casein micelles strictly behave as hard spheres in a liquid; meaning that they are still separated from each other and interact through excluded volume effects only.[38] The maximum concentration of 180 g·L^{-1} corresponds to a volume fraction ϕ = 0.78. This last value exceeds the random close packing limit for monodisperse hard spheres (ϕ_{cp} = 0.64) simply because the casein micelles are 30−40% polydisperse spheres that can pack more efficiently than monodisperse ones. Also, the fact that the micelles interact through excluded volume effects only is explained by the high ionic strength of the dispersion (= low if not inexistent electrostatic repulsions) and the absence of brush repulsion forces as long as there is no direct contact between two neighboring micelles. In such "nonrepulsive" situations, the osmotic pressure is directly related to the total number n of species in the dispersion according to the Van't Hoff's law

$$\Pi = \frac{n}{V}RT \tag{25}$$

This simple relation readily explains the linear dependence of Π with casein concentration C. In addition, we can show that n not only counts the total number of casein micelles in the dispersions, but also counts some small peptides and casein

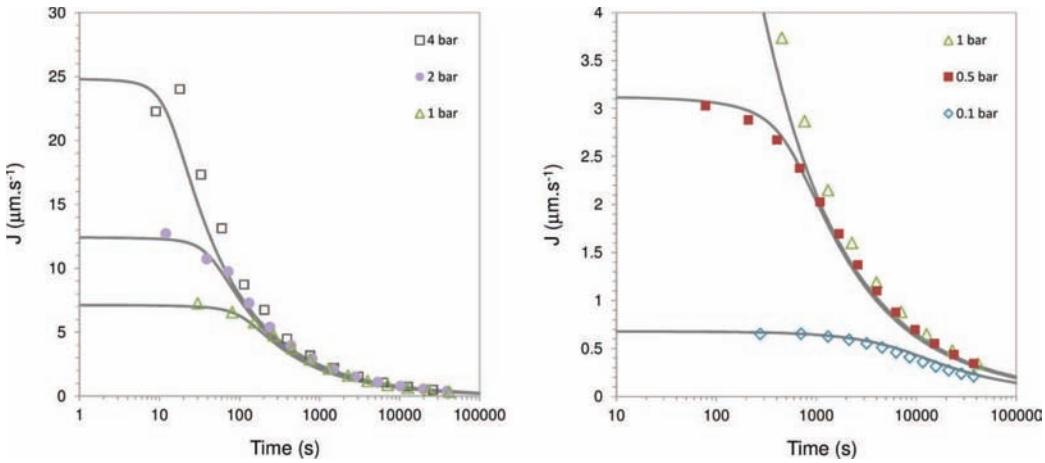

Figure 5. Evolution of permeation flux J as a function of time for dead-end ultrafiltrations of NPC dispersions at different transmembrane pressures. The symbols are the experimental data. The lines are the predictions obtained using the filtration model (procedure of section 2.2) and assuming that Π and k evolves with C according to eqs 26 and 28, respectively. The results are presented in a semilog plot to better visualize the data at small filtration times.

fragments that are in fact retained by the dialysis membrane during osmotic stress (see ref 9 for a detailed discussion). Those small species are initially present in the NPC powder at a very low mass concentration. Their number density is, however, very high. Also, when the powder is dispersed in an aqueous solvent, their number density increases with time as a result of proteolysis, this phenomenon being due to the presence of a small amount of enzymes (plasmin) in the NPC powder. This is demonstrated here by the fact that higher osmotic pressures are measured for a NPC dispersions aged of 14 days (Figure 4; quite consistently, these pressures also exactly correspond to the pressure measured using osmotic stress after 14 days of dialysis).

In the concentrated to very dense concentration regime ($C >$ 180 g·L^{-1}), the osmotic pressure rises approximately as the sixth power of concentration (Figure 4). Phase transition actually occurs at the entry of this regime, and the samples all behave as coherent solids or gels in this concentration range.[9,38] This phase transition is due to direct interactions between the casein micelles when they are forced to get into close contact, i.e., when ϕ exceeds 0.78. As concentration is further increased, the casein micelles are forced to deform and de-swell. Effective volume fractions superior to 1 are reached, clearly indicating that the micelles have shrunk to a lower volume. In this second concentration regime, and in direct contrast to the first regime, the osmotic pressure is related to the strong interactions between (= surface interactions) and inside (= compression resistance) the casein micelles.[9] It is because such strong and direct interactions are involved that the osmotic pressure rises so fast with casein concentration. This also implies that the contribution of the small species to the osmotic pressure can be totally neglected in this second regime.

Altogether, the results of Figure 4 can be used to obtain an analytical expression for the evolution of Π with C. In our case, we are interested in the $\Pi(C)$ relation for a "fresh" dispersion of casein micelles, as we aim to build a filtration model for this very case. We choose the following expression, which is a simple polynomial function that fits our data in a very acceptable manner (Figure 4)

$$\Pi(\text{Pa}) = aC + bC^2 + cC^3 + fC^6 \tag{26}$$

with C expressed in g·L^{-1}, $a = 8$, $b = 3 \times 10^{-2}$, $c = 1 \times 10^{-5}$, and $f = 3 \times 10^{-11}$.

4.2. Permeability *k*(*C*). The permeability $k(C)$ of the NPC dispersions was estimated using two different approaches. The first approach lies on the reverse calculation of $k(C)$ using the filtration model of section 2 and following the procedure detailed in section 2.3. For this purpose, the evolution of Π versus C is needed, which is the eq 26 we just determined. Some filtration data are also required to make the calculations (see eq 19). We report the data used in our case in Figure 5. Those results correspond to five dead-end filtration experiments performed at transmembrane pressures ranging from 0.1 to 4 bar. The resulting values of k are given in Figure 6. The second approach consists of measuring k by monitoring the kinetics of compression in osmotic stress experiments. Four experiments of this type were performed. The k values are also reported in Figure 6.

A first and quite reassuring remark is that the k points (Figure 6), despite being obtained in different pressure conditions and/or with different techniques, appear to be distributed over one single curve. This curve covers 4 decades of k values, with a permeability that decreases with C in a monotonous way. As for the osmotic pressure, we then propose to discuss these results by considering two concentration regimes.

Before Close-Packing/Dilute Regime ($C <$ 180 g·L^{-1}). In this first regime, and as already explained, the micelles are still separated from each other, meaning that there is still plenty of interstitial space between them where liquid can flow. In that case, it seems judicious to compare our results with the predictions for a system of hard and nonporous spheres. The permeability of such a dispersion can be estimated from the Happel's equation[36]

$$k_{\text{Happel}} = \frac{2r_p^2}{9\phi}\frac{6 - 9\phi^{1/3} + 9\phi^{5/3} - 6\phi^2}{6 + 4\phi^{5/3}} \tag{27}$$

with r_p the radius of the involved particles and ϕ the volume fraction occupied by the particles. Taking the voluminosity of the casein micelle and an average particle radius of 50 nm,[5] we obtain the dashed curved of Figure 6 (Happel (1)). In the

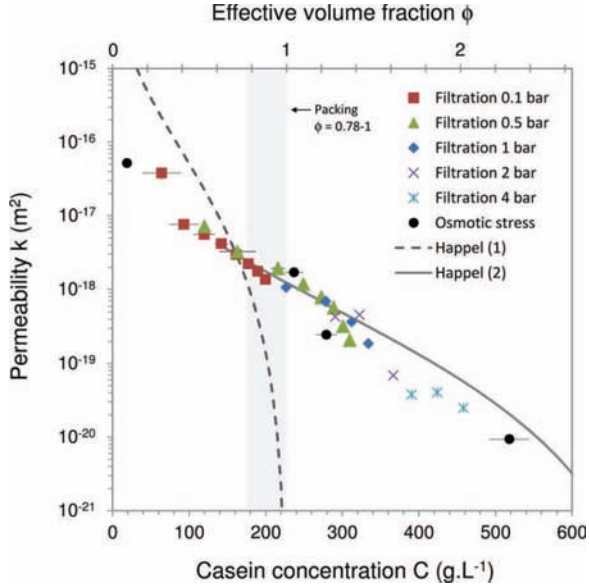

Figure 6. Evolution of the permeability k of the NPC dispersions as a function of casein concentration and effective volume fraction. Those k values were obtained both from osmotic stress experiments (closed circles) and from the filtration data of Figure 5 using the procedure of section 2.3 (other symbols). The shaded area gives the region where phase transition occurs; which corresponds to a packing fraction ϕ between 0.78 and 1 (180−230 g·L^{-1}, eq 24 with voluminosity v = 4.4 mL.g^{-1}).[9,38,58] The results are compared with the permeability of monodisperse nonporous hard sphere dispersions as calculated from the theoretical expression of Happel (eq 27): Happel (1) (dashed line) = objects of 100 nm in diameter and voluminosity v = 4.4 mL.g^{-1}, Happel (2) (full line) = objects of 8.8 nm in diameter and v = 1.4 mL.g^{-1}.

concentration regime that we consider here, we clearly see that all the measured permeabilities are lower than the prediction for hard spheres. As the Happel's approximation is for nonpermeable and monodisperse hard-spheres, two possible reasons come to mind for explaining this difference: (i) the size polydispersity of the micelles; (ii) the porosity of the micelles. However, if we now look at the theory, we can actually demonstrate that none of these reasons are in fact valid. The effect of polydispersity on the permeability of a bed of hard spheres has been investigated in the work of Li and Park.[59] These authors show that a broad distribution of size, as in the case of casein micelle,[5,6] indeed leads to a lower permeability as compared to the monodisperse case. However, this effect is relatively tenuous, and cannot explain the large difference that we observe. The effect of porosity is even less equivocal. Indeed, theoretical works have clearly demonstrated that dispersions of porous spheres always have higher permeabilities than dispersions of nonporous spheres of the same size.[30,50] So as the properties of the casein micelle alone do not seem to explain our results, we speculate that the low permeabilities we measure are partly due to other species present in the dispersions, those species being the small peptides and casein fragments that are already responsible for the high osmotic pressures measured at low casein concentration.[9] Of course, this is only a qualitative assessment at that point, which would need to be verified in future studies.

After Close-Packing/Dense Regime (C > 180 g·L^{-1}). At the entry of this regime (packing zone, ϕ = 0.78−1), the permeability of the hard sphere system diverges toward zero (dashed line, Figure 6). This is readily explained by the fact that the interstitial spaces between the spheres are progressively closed. On the other hand, the permeability of the NPC system does not diverge at all, and still continues to slowly and regularly decrease with C. This is a direct effect of the internal porosity of the micelle as compared to nonporous hard spheres: the fluid gets forced through the micelle as the intermicellar voids are progressively closed. (As a side-effect, we can reasonably assume that the contribution of the small species to k tends to become negligible when reaching such high volume occupancy.) After close-packing, and especially at sufficiently high concentrations where ϕ > 1, the dispersion turns into a cohesive gel in which the micelles are in direct contact and "squeezed" against each other. If we assume that the gel is homogeneous and lacks microfractures or other local heterogeneities, the permeability of the system is then entirely determined by the internal structure and porosity of the casein micelle itself. In that case, it is difficult to compare our results with theoretical expressions for porous systems, especially because we are still lacking the fine structural details that would be necessary to inject in such models (internal tortuosity? presence or not of internal voids? Mesh size of the casein network?). However, there is one very simplified model that can be tested, and that we already used for explaining the osmotic pressure of the casein micelle in the very dense regime.[9] In this model, the micelle interior is described as a collection of nonconnected hard spheres that occupy a fraction ϕ of the total volume of the micelle. Still using the Happel expression, and by taking the size (r_p = 4.4 nm) and the voluminosity (v = 1.4 mL.g^{-1}) of these substructures as identical to those used in our previous paper, we obtain the dashed gray curve of Figure 6. One can see that the correspondence with our experimental results is quite good. Of course, this view of a micelle composed of noninteracting spheres cannot be taken as realistic. There is however a certain physical meaning behind the use of such a model. We refer the reader to a previous paper for a detailed discussion on that point.[9]

Empirical Equation for k(C). One important objective of section 4.2 is to obtain an empirical expression for k versus C. This expression is then used for modeling the filtration of NPC dispersions (next section). We propose to employ the following function, drawn in Figure 7

$$k(\mathrm{m}^2) = \frac{1}{a'C + b'C^2 + f'C^6} \tag{28}$$

with C expressed in g·L^{-1}, a' = 9.2 × 10^{14}, b' = 1.1 × 10^{12}, and f' = 4.6 × 10^3.

Note that this expression is based on the fact that k varies with C in a fashion that is quite similar to that of Π with C (slope of ±1 at low concentrations, and slope of ±6 at high concentrations). Such a similarity between Π and k may be fortuitous, or may have a physical explanation. We do not have an answer to this question yet.

4.3. Analysis of the Resulting Filtration Model. Now that we have two analytical expressions for $\Pi(C)$ and $k(C)$, we can build and use the filtration model of section 2. A first test of the model consists of predicting the filtration fluxes for the conditions of the filtration runs we already performed (Figure 5). For that purpose, we use the procedure given in section 2.2 and the adequate values of transmembrane pressure, casein concentration, and membrane resistance. The fluxes obtained

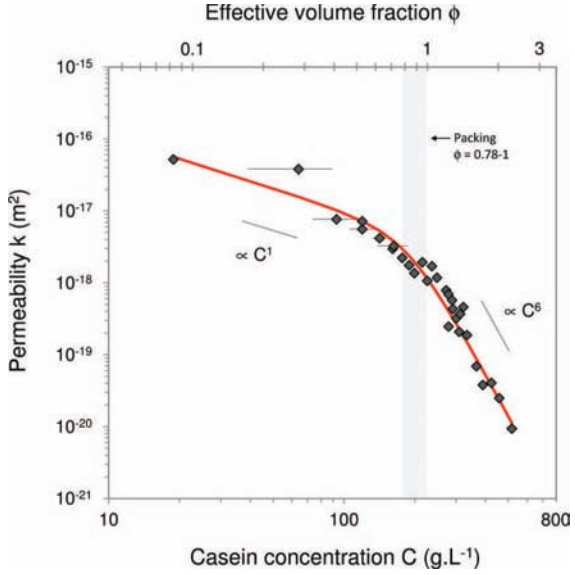

Figure 7. Empirical expression for $k(C)$. The symbols are the experimental data. The full line is eq 28.

are shown in Figure 5 as full lines. One sees that the correspondence between the model and the experimental data is very satisfactory. Of course, we are not doing a "validation" of the model here as the experimental data of Figure 5 are the values we used to build the model. However, this test is useful because it shows that the analytical expression chosen for $k(C)$ efficiently captures the "true" variation of permeability over the entire range of concentration investigated during the filtration (from 1 g·L^{-1} in the bulk to the maximum concentration that can be attained at the membrane surface, i.e, almost 500 g·L^{-1} at ΔP = 4 bar). Incidentally, this test also shows that we did not make any mistake in deriving and using the equations given in section 2.

To analyze the physics of the local accumulation of casein micelles, let us now consider the "virtual" dead-end filtration of a NPC dispersion with C_{bulk} = 1 g·L^{-1}; the membrane resistance being arbitrarily set to $R_m = 1 \times 10^{13}$ m^{-1}. For a given transmembrane pressure ΔP, the model is not only able to predict the flux versus time, but can also give the evolution of the osmotic pressure Π_m at the membrane surface versus time. This is what we do in Figure 8, where both J and Π_m are plotted against time for three values of ΔP. Π_m can in turn be compared to the critical osmotic pressure Π_{crit}, i.e., the pressure at which phase transition occurs (Figure 1). In a recent paper,

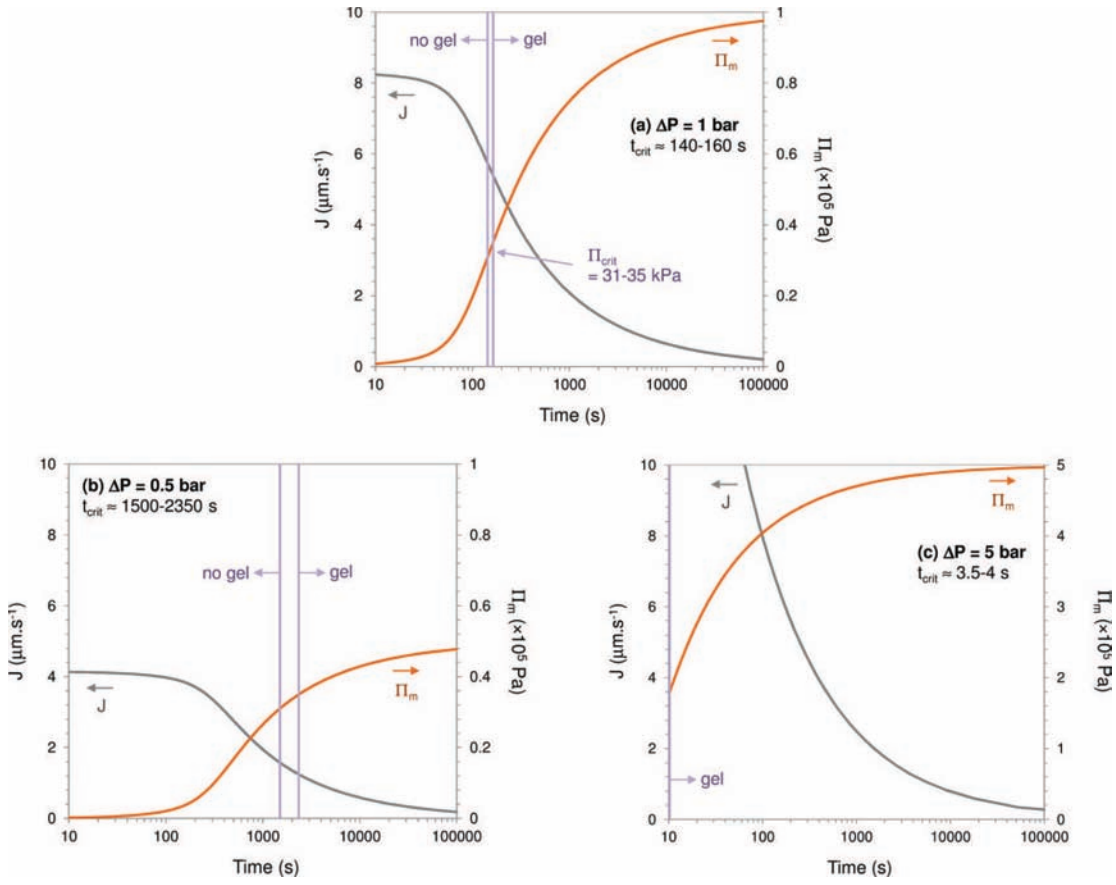

Figure 8. Using the model: time dependence of J and Π_m for "virtual" filtrations of a NPC dispersion. For all cases, the bulk casein concentration was set to C_{bulk} = 1 g·L^{-1} and the membrane resistance was set to $R_m = 1 \times 10^{13}$ m^{-1}. The three figures (a)−(c) correspond to three different transmembrane pressures. All calculations were made following the procedure of section 2.2, and assuming that Π and k evolve with C according to eqs 26 and 28, respectively. In all figures, the approximate time t_{crit} at which Π_m reaches the critical value for phase transition (Π_{crit} = 31−35 kPa, see ref 40) is indicated with vertical full lines.

we were able to measure this pressure for NPC dispersions, and we found Π_{crit} = 31−35 kPa.[40] From that value, it is possible to evaluate the filtration time at which an irreversible deposit is formed at the membrane surface. Knowing this critical time t_{crit} is of crucial importance for whoever wants to avoid any severe fouling of the filtration installation and minimize cleaning costs.

Of course, and as illustrated in Figure 8, t_{crit} depends on the applied transmembrane pressure. At ΔP = 1 bar (Figure 8a), a deposit is formed after only 2 min of filtration. At ΔP = 5 bar (Figure 8c), the formation of the deposit is almost instantaneous with t_{crit} = 3.5−4 s (!). At ΔP = 0.5 bar (Figure 8b), which seems to be a good compromise, the filtration can be conducted during 30 min before a gel is formed onto the membrane. Thus, by performing successive filtrations at ΔP = 0.5 bar and for less than 30 min, it is theoretically possible to conduct the filtration on an ″infinite″ time interval, without the annoying formation of an irreversible deposit at the membrane. The only constraint would be to ″redisperse″ the polarized layer between each run, by a simple agitation procedure, for instance (like in ref 40).

Figure 9 gives another illustration of how the filtration model can be used. For given conditions of filtration (taken as identical to those of Figure 8a in that case), it is indeed possible to calculate the casein concentration profile at the membrane surface for a given filtration time. In the conditions of Figure 9, we see that the thickness of the accumulated layer reaches about 10 μm at relatively short times (see the profile at t = 128 s). It takes more than 2 days for this layer to reach 0.5 mm in thickness. At this point, the gel is about 50 μm thick, which represents up to 10% of the total thickness of the accumulated layer.

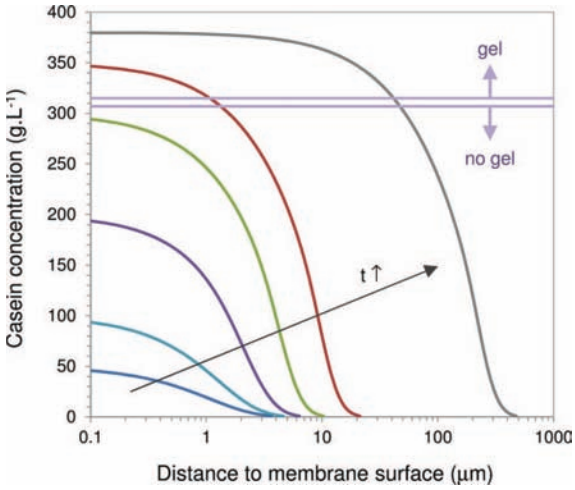

Figure 9. Modeling the casein concentration profile in the accumulated layer during a ″virtual″ filtration of a NPC dispersion. The case shown here corresponds to the conditions of Figure 8a: C_{bulk} = 1 g·L^{-1}, R_m = 1 × 10^{13} m^{-1}, ΔP = 1 bar. Filtration times from bottom to top: 6 s, 14 s, 43 s, 128 s, 456 s, 2.3 d.

In Figure 10, we finally compare the predictions of our model to the interesting results of David et al.[60] In contrast to the first modeling tests of Figure 5, the idea is now to directly confront our model to experimental data that it has never ″seen″ before. The study of David et al. is particularly suitable to that purpose because (i) they also investigate NPC dispersions of casein micelles, and (ii) their filtration results include filtration fluxes and concentration profiles at the membrane surface, such measurements being made possible via combined filtration/SAXS experiments.

Figure 10a gives the prediction of flux versus time as compared to the data of David et al. The agreement is acceptable, with predicted fluxes that are in the same range as those measured during the filtration, particularly at intermediate times (1000−10000 s). Figure 10b gives the experimental and the predicted concentration profiles. Again, the agreement is acceptable, with predictions that do not exactly match the experimental concentrations, but which are clearly close to them.

In fact, several reasons could be responsible for the small—but existing—differences between our model and the experimental data of David et al. The principal are as follows:

Water instead of UF permeate: David et al. prepared their dispersions by mixing the NPC powder with pure water instead of UF permeate. In such dispersions, the casein micelles have characteristics that are close to native, but with some minor changes in size (−5%) and mineral composition (−7% in calcium and phosphate content).[54] It is imaginable that such changes have some effects on $\Pi(C)$ and $k(C)$, making eqs 26 and 28 not totally appropriate to this case.

A 100 kD membrane: All our filtration, osmotic stress, and osmometry experiments were performed with membranes of ∼10 kD. Conversely, David et al. used a 100 kD membrane for their filtrations. In their case, it is probable that the 100 kD membrane does not retain some of the small species that are retained by the 10 kD filtration and dialysis membranes. Again, that would have a potential impact on the $\Pi(C)$ and $k(C)$ curves that need to be used for modeling the David's results, making eqs 26 and 28 not fully appropriate.

SAXS calibration: In the setup used by David et al., the casein concentration at the vicinity of the membrane is measured using an X-ray beam of 70 μm high (i.e., in the direction perpendicular to the membrane).[60] As a consequence, and despite all the precautions that the authors employ to calibrate the position of the beam relative to the membrane surface, we cannot exclude that an error of a few micrometers or even a few dozen micrometers exists between the positions given by the authors and the ″exact″ positions of the given concentration points. To illustrate the effect of such a small experimental error, we report in Figure 10c the experimental points of David et al. with a shift of 40 μm toward lower x values. In that case, one can see that the correspondence between the model and the experiment is very good.

Having listed all these points, it now seems clear that the ″acceptable″ agreement of Figures 10a and b is in fact extremely satisfactory. So it appears that the model (and its associated $\Pi(C)$ and $k(C)$ functions) is able to accurately predict the dead-end filtration of casein micelle dispersions in given conditions of transmembrane pressure and casein concentration.

If we now look at the casein micelle as a model object, such successful results make us confident that the modeling approach proposed here could be generalized to any ″complicated″ colloidal dispersion of soft and/or permeable and/or polydisperse objects.

5. CONCLUSION

Colloids have always been problematic objects in membrane filtration, essentially because their overconcentration at the membrane surface strongly impacts the performance of the

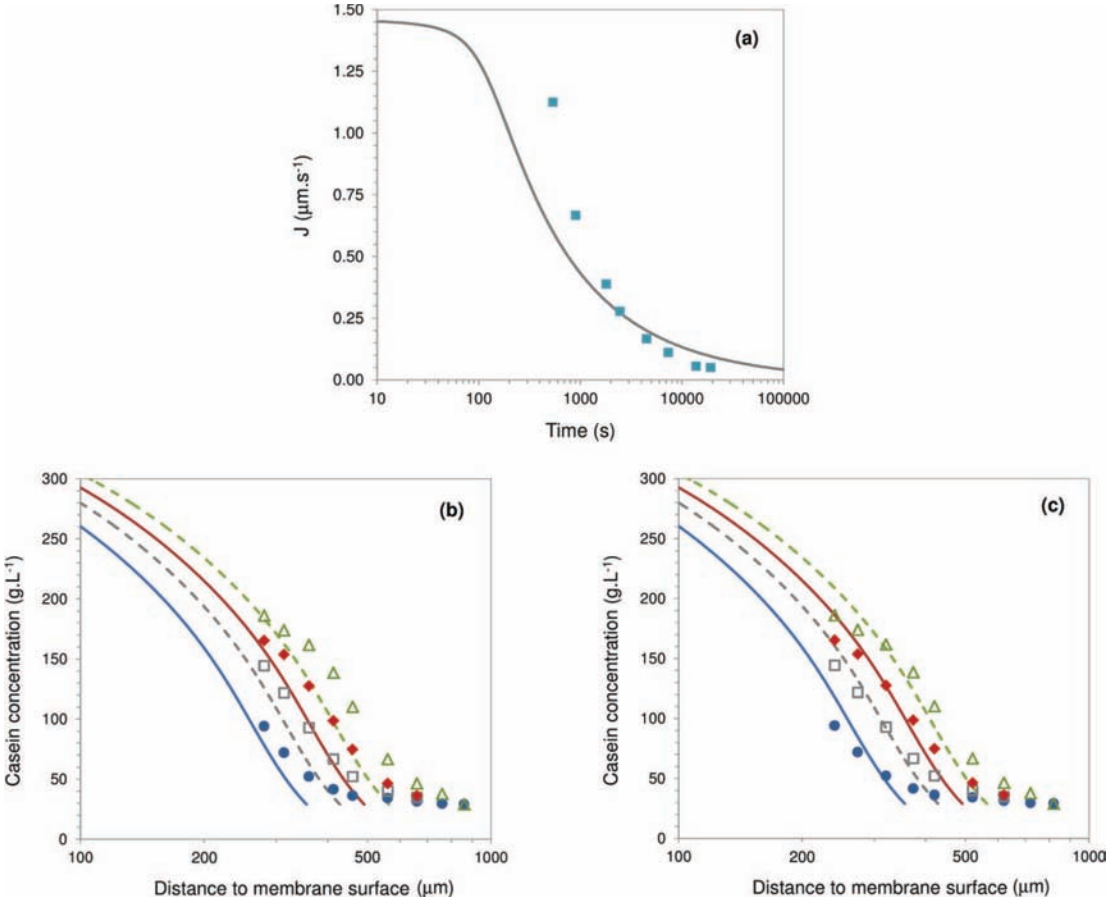

Figure 10. Comparing the model predictions with actual filtration results: filtration flux versus time (a), casein concentration profiles in the accumulated layer (b)−(c). The experimental results (symbols) are taken from the work of David et al.,[60] where a dispersion of NPC powder dispersed in water was filtered through a 100 kD ultrafiltration membrane at ΔP = 1.2 bar. The full and dashed lines are the predictions obtained from the filtration model of section 2.2, assuming that Π and k evolve with C according to eqs 26 and 28. In (b) and (c), the filtration times from bottom to top are: 133, 188, 246, and 325 min. In (c), the experimental results are reported supposing that the distances given in the original David's paper are overestimated by 40 μm.

process.[17] However, after some years of development, "colloidal" filtration models now exist.[1,32] But still, they are limited to the ideal case of monodisperse hard-sphere colloids, which makes them impractical in the real world. In this paper, we treat the problem of soft and permeable colloids, with the objective of proposing a general approach for predicting the filtration of such objects.

For that purpose, and for a number of reasons that we give in the Introduction, we chose to base our study on the specific case of milk filtration, all experiments being performed with dispersions of milk casein micelles. Using this example, we develop the general idea that a filtration model can always be built for a given colloidal dispersion as long as this dispersion has been characterized in terms of osmotic pressure Π and hydraulic permeability k. Following what was already proposed for hard-sphere colloids, the filtration model can then be constructed knowing the evolution of Π and k with the colloid concentration.

For colloids that are soft, deformable, and permeable, the major issue is that the permeability of the dispersion cannot be assessed in a trivial way like in the case for hard-sphere colloids. To get around this difficulty, we followed two distinct approaches to actually measure the permeability k: a direct approach, involving osmotic stress experiments, and a "reverse calculation" approach, consisting of estimating k through well-controlled filtration experiments.

The reported evolution of $k(C)$ is the first important result of this paper, as such experimental data have rarely been reported until now for such peculiar objects (in contrast to theoretical studies that are already available[30,50]). We briefly discuss this evolution in light of our previous studies about the osmotic and phase properties of casein micelle dispersions.[5,9,38] We also show that some questions remain, such as the exact effect of the presence of small impurities on k, or the potential physical basis of the observed similarities between the evolution of Π and k with C.

From the knowledge of $k(C)$, we then construct a filtration model and analyze it through a series of test and "virtual" experiments. We also directly compare the predictions of the model to filtration data obtained by other authors in combined filtration/SAXS experiments. In our opinion, the results of those calculations and comparisons are quite unequivocal and totally validate our methodology.

ASSOCIATED CONTENT

Supporting Information

A note on the equivalence between the modeling approach proposed in this paper and the well-known convection−diffusion equation in the case of a dispersion of monodisperse hard sphere colloids. This material is available free of charge via the Internet at http://pubs.acs.org.

AUTHOR INFORMATION

Corresponding Author

*E-mail: Antoine.Bouchoux@insa-toulouse.fr.

Present Address

[⊥]Laboratoire d'Ingénierie des Systèmes Biologiques et des Procédés / LISBP, UMR 5504/792 INRA-CNRS-INSA, 135 avenue de Rangueil, 31077 Toulouse cedex 04, France.

Notes

The authors declare no competing financial interest.

ACKNOWLEDGMENTS

The authors acknowledge the financial support provided by the Institut National de la Recherche Agronomique (INRA) and Région Bretagne.

REFERENCES

(1) Bowen, W. R.; Williams, P. M. Quantitative predictive modelling of ultrafiltration processes: Colloidal science approaches. *Adv. Colloid Interface Sci.* **2007**, *134−135*, 3−14.

(2) Tan, B. H.; Tam, K. C. Review on the dynamics and microstructure of pH-responsive nano-colloidal systems. *Adv. Colloid Interface Sci.* **2008**, *136*, 25−44.

(3) Mattsson, J.; Wyss, H. M.; Fernandez-Nieves, A.; Miyazaki, K.; Hu, Z.; Reichman, D. R.; Weitz, D. A. Soft colloids make strong glasses. *Nature* **2009**, *462*, 83−86.

(4) Dalgleish, D. G. On the structural models of bovine casein micelles-review and possible improvements. *Soft Matter* **2011**, *7*, 2265−2272.

(5) Bouchoux, A.; Gésan-Guiziou, G.; Pérez, J.; Cabane, B. How to squeeze a sponge: casein micelles under osmotic stress, a SAXS study. *Biophys. J.* **2010**, *99*, 3754−3762.

(6) De Kruif, C. G. Supra-aggregates of casein micelles as a prelude to coagulation. *J. Dairy Sci.* **1998**, *81*, 3019−3028.

(7) Ouanezar, M.; Guyomarc'h, F.; Bouchoux, A. AFM imaging of milk casein micelles: Evidence for structural rearrangement upon acidification. *Langmuir* **2012**, *28*, 4915−4919.

(8) Dalgleish, D. G.; Corredig, M. The structure of the casein micelle of milk and its changes during processing. *Annu. Rev. Food Sci. Technol.* **2012**, *3*, 449−467.

(9) Bouchoux, A.; Cayemitte, P. E.; Jardin, J.; Gésan-Guiziou, G.; Cabane, B. Casein micelle dispersions under osmotic stress. *Biophys. J.* **2009**, *96*, 693−706.

(10) Gebhardt, R.; Vendrely, C.; Kulozik, U. Structural characterization of casein micelles: shape changes during film formation. *J. Phys.: Condens. Matter* **2011**, *23*, 444201.

(11) Maubois, J. L.; Ollivier, G. In *Foods proteins and their applications*; Damodaran, S., Paraf, A., Eds.; Marcel Dekker: New York, 1997; pp 579−595.

(12) Brans, G.; Schroen, C. G. P. H.; Van Der Sman, R. G. M.; Boom, R. M. Membrane fractionation of milk: state of the art and challenges. *J. Membr. Sci.* **2004**, *243*, 263−272.

(13) Jimenez-Lopez, A. J. E.; Leconte, N.; Garnier-Lambrouin, F.; Bouchoux, A.; Rousseau, F.; Gésan-Guiziou, G. Ionic strength dependence of skimmed milk microfiltration: Relations between filtration performance, deposit layer characteristics and colloidal properties of casein micelles. *J. Membr. Sci.* **2011**, *369*, 404−413.

(14) Cohen, R. D.; Probstein, R. F. Colloidal fouling of reverse osmosis membranes. *J. Colloid Interface Sci.* **1986**, *114*, 194−207.

(15) Belfort, G.; Davis, R. H.; Zydney, A. L. The behavior of suspensions and macromolecular solutions in crossflow microfiltration. *J. Membr. Sci.* **1994**, *96*, 1−58.

(16) Bowen, W. R.; Jenner, F. Dynamic ultrafiltration model for charged colloidal dispersions: A Wigner-Seitz cell approach. *Chem. Eng. Sci.* **1995**, *50*, 1707−1736.

(17) Bacchin, P.; Aimar, P.; Field, R. W. Critical and sustainable fluxes: Theory, experiments and applications. *J. Membr. Sci.* **2006**, *281*, 42−69.

(18) Chen, J. C.; Elimelech, M.; Kim, A. S. Monte Carlo simulation of colloidal membrane filtration: Model development with application to characterization of colloid phase transition. *J. Membr. Sci.* **2005**, *255*, 291−305.

(19) Elimelech, M.; Bhattacharjee, S. A novel approach for modeling concentration polarization in crossflow membrane filtration based on the equivalence of osmotic pressure model and filtration theory. *J. Membr. Sci.* **1998**, *145*, 223−241.

(20) Tang, C. Y.; Chong, T. H.; Fane, A. G. Colloidal interactions and fouling of NF and RO membranes: A review. *Adv. Colloid Interface Sci.* **2011**, *164*, 126−143.

(21) Kim, S.; Marion, M.; Jeong, B. H.; Hoek, E. M. V. Crossflow membrane filtration of interacting nanoparticle suspensions. *J. Membr. Sci.* **2006**, *284*, 361−372.

(22) Vollebregt, H. M.; Van Der Sman, R. G. M.; Boom, R. M. Suspension flow modelling in particle migration and microfiltration. *Soft Matter* **2010**, *6*, 6052−6064.

(23) Bacchin, P.; Meireles, M.; Aimar, P. Modelling of filtration: from the polarised layer to deposit formation and compaction. *Desalination* **2002**, *145*, 139−146.

(24) Bowen, W. R.; Mongruel, A.; Williams, P. M. Prediction of the rate of crossflow membrane ultrafiltration: a colloidal interaction approach. *Chem. Eng. Sci.* **1996**, *51*, 4321−4333.

(25) Bonnet-Gonnet, C.; Belloni, L.; Cabane, B. Osmotic pressure of latex dispersion. *Langmuir* **1994**, *10*, 4012−4021.

(26) Carrière, D.; Page, M.; Dubois, M.; Zemb, T.; Colfen, H.; Meister, A.; Belloni, L.; Schonhoff, M.; Mohwald, H. Osmotic pressure in colloid science: clay dispersions, catanionics, polyelectrolyte complexes and polyelectrolyte multilayers. *Colloids Surf., A* **2007**, *303*, 137−143.

(27) Jönsson, B.; Persello, J.; Li, J.; Cabane, B. Equation of State of Colloidal Dispersions. *Langmuir* **2011**, *27*, 6606−6614.

(28) Menut, P.; Seiffert, S.; Sprakel, J.; Weitz, D. A. Does size matter? Elasticity of compressed suspensions of colloidal- and granular-scale microgels. *Soft Matter* **2012**, *8*, 156−164.

(29) Carman, P. C. Fluid flow through granular beds. *Chem. Eng. Res. Des.* **1997**, *75*, S32−S48.

(30) Deo, S.; Filippov, A.; Tiwari, A.; Vasin, S.; Starov, V. Hydrodynamic permeability of aggregates of porous particles with an impermeable core. *Adv. Colloid Interface Sci.* **2011**, *164*, 21−37.

(31) Petsev, D. N.; Starov, V. M.; Ivanov, I. B. Concentrated dispersions of charged colloidal particles: Sedimentation, ultrafiltration and diffusion. *Colloids Surf., A* **1993**, *81*, 65−81.

(32) Bacchin, P.; Si-Hassen, D.; Starov, V.; Clifton, M. J.; Aimar, P. A unifying model for concentration polarization, gel-layer formation and particle deposition in cross-flow membrane filtration of colloidal suspensions. *Chem. Eng. Sci.* **2002**, *57*, 77−91.

(33) Merlin, A.; Salmon, J. B.; Leng, J. Microfluidic-assisted growth of colloidal crystals. *Soft Matter* **2012**, *8*, 3526−3537.

(34) Bacchin, P.; Espinasse, B.; Bessière, Y.; Fletcher, D. F.; Aimar, P. Numerical simulation of colloidal dispersion filtration: description of critical flux and comparison with experimental results. *Desalination* **2006**, *192*, 74−81.

(35) Bessiere, Y.; Fletcher, D. F.; Bacchin, P. Numerical simulation of colloid dead-end filtration: Effect of membrane characteristics and operating conditions on matter accumulation. *J. Membr. Sci.* **2008**, *313*, 52−59.

(36) Happel, J. Viscous flow in multiparticle systems: Slow motion of fluids relative to beds of spherical particles. *AIChE J.* **1958**, *4*, 197−201.

(37) Bowen, W. R.; Williams, P. M. Obtaining the osmotic pressure of electrostatically stabilized colloidal dispersions from frontal ultrafiltration experiments. *J. Colloid Interface Sci.* **2001**, *233*, 159−163.
(38) Bouchoux, A.; Debbou, B.; Gesan-Guiziou, G.; Famelart, M. H.; Doublier, J. L.; Cabane, B. Rheology and phase behavior of dense casein micelle dispersions. *J. Chem. Phys.* **2009**, *131*, 165106−165111.
(39) Nair, P. K.; Dalgleish, D. G.; Corredig, M. Colloidal properties of concentrated heated milk. *Soft Matter* **2013**, *9*, 3815−3824.
(40) Qu, P.; Gésan-Guiziou, G.; Bouchoux, A. Dead-end filtration of sponge-like colloids: The case of casein micelle. *J. Membr. Sci.* **2012**, *417*−*418*, 10−19.
(41) Wijmans, J. G.; Nakao, S.; Van Den Berg, J. W. A.; Troelstra, F. R.; Smolders, C. A. Hydrodynamic resistance of concentration polarization boundary layers in ultrafiltration. *J. Membr. Sci.* **1985**, *22*, 117−135.
(42) Tiller, F. M.; Kwon, J. H. Role of porosity in filtration: XIII. Behavior of highly compactible cakes. *AIChE J.* **1998**, *44*, 2159−2167.
(43) Sherwood, J. D. Initial and final stages of compressible filtercake compaction. *AIChE J.* **1997**, *43*, 1488−1493.
(44) Lee, D. J.; Wang, C. H. Theories of cake filtration and consolidation and implications to sludge dewatering. *Water Res.* **2000**, *34*, 1−20.
(45) Rubinstein, M.; Colby, R. H.; Dobrynin, A. V.; Joanny, J. F. Elastic modulus and equilibrium swelling of polyelectrolyte gels. *Macromolecules* **1996**, *29*, 398−406.
(46) Style, R. W.; Peppin, S. S. L. Crust formation in drying colloidal suspensions. *Proc. R. Soc. London, Ser. A* **2011**, *467*, 174−193.
(47) Bowen, W. R.; Jenner, F. Electroviscous effects in charged capillaries. *J. Colloid Interface Sci.* **1995**, *173*, 388−395.
(48) Bowen, W. R.; Williams, P. M. The osmotic pressure of electrostatically stabilized colloidal dispersions. *J. Colloid Interface Sci.* **1996**, *184*, 241−250.
(49) Parsegian, V. A.; Rand, R. P.; Fuller, N. L.; Rau, D. C. Osmotic stress for the direct measurement of intermolecular forces. *Method. Enzymol.* **1986**, *127*, 400−416.
(50) Abade, G. C.; Cichocki, B.; Ekiel-Jezewska, M. L.; Nagele, G.; Wajnryb, E. Diffusion, sedimentation, and rheology of concentrated suspensions of core-shell particles. *J. Chem. Phys.* **2012**, *136*, 104902−104916.
(51) Schuck, P.; Piot, M.; Méjean, S.; Le Graët, Y.; Fauquant, J.; Brulé, G.; Maubois, J. L. Spray-drying of native phosphocaseinate obtained by membrane microfiltration. *Lait* **1994**, *74*, 375−388.
(52) Jenness, R.; Koops, J. Preparation and properties of a salt solution which simulates milk ultrafiltrate. *Neth. Milk Dairy J.* **1962**, *16*, 153−164.
(53) Gaiani, C.; Scher, J.; Schuck, P.; Hardy, J.; Desobry, S.; Banon, S. The dissolution behavior of native phosphocaseinate as a function of concentration and temperature using a rheological approach. *Int. Dairy J.* **2006**, *16*, 1427−1434.
(54) Famelart, M. H.; Lepesant, F.; Gaucheron, F.; Le Graet, Y.; Schuck, P. pH-induced physicochemical modifications of native phosphocaseinate suspensions: influence of aqueous phase. *Lait* **1996**, *76*, 445−460.
(55) Moitzi, C.; Menzel, A.; Schurtenberger, P.; Stradner, A. The pH induced sol-gel transition in skim milk revisited. A detailed study using time-resolved light and X-ray scattering experiments. *Langmuir* **2011**, *27*, 2195−2203.
(56) Tuinier, R.; De Kruif, C. G. Stability of casein micelles in milk. *J. Chem. Phys.* **2002**, *117*, 1290−1295.
(57) http://lpsb.nichd.nih.gov/osmotic_stress.htm, Accessed July 2013.
(58) Dahbi, L.; Alexander, M.; Trappe, V.; Dhont, J. K. G.; Schurtenberger, P. Rheology and structural arrest of casein suspensions. *J. Colloid Interface Sci.* **2010**, *342*, 564−570.
(59) Li, Y.; Park, C. W. Permeability of packed beds filled with polydisperse spherical particles. *Ind. Eng. Chem. Res.* **1998**, *37*, 2005−2011.
(60) David, C.; Pignon, F.; Narayanan, T.; Sztucki, M.; Gesan-Guiziou, G.; Magnin, A. Spatial and temporal in situ evolution of the concentration profile during casein micelle ultrafiltration probed by small-angle X-ray scattering. *Langmuir* **2008**, *24*, 4523−4529.